



**HAL**  
open science

## Reusable molecularly imprinted polymeric nanospheres for diclofenac removal from water samples

Noha Amaly, Georges Istamboulie, Ahmed Y El-Moghazy, Thierry Noguer

### ► To cite this version:

Noha Amaly, Georges Istamboulie, Ahmed Y El-Moghazy, Thierry Noguer. Reusable molecularly imprinted polymeric nanospheres for diclofenac removal from water samples. *Journal of Chemical Research*, 2021, 45 (1-2), pp.102-110. <10.1177/1747519820925998>. <hal-04082182>

**HAL Id: hal-04082182**

**<https://hal.science/hal-04082182v1>**

Submitted on 26 Apr 2023

HAL is a multi-disciplinary open access archive for the deposit and dissemination of scientific research documents, whether they are published or not. The documents may come from teaching and research institutions in France or abroad, or from public or private research centers.

L'archive ouverte pluridisciplinaire HAL, est destinée au dépôt et à la diffusion de documents scientifiques de niveau recherche, publiés ou non, émanant des établissements d'enseignement et de recherche français ou étrangers, des laboratoires publics ou privés.



Distributed under a Creative Commons CC BY-NC 4.0 - Attribution - Non-commercial use - International License

# Reusable molecularly imprinted polymeric nanospheres for diclofenac removal from water samples

Journal of Chemical Research  
January-February 2021: 102–110  
© The Author(s) 2020  
Article reuse guidelines:  
sagepub.com/journals-permissions  
DOI: 10.1177/1747519820925998  
journals.sagepub.com/home/chl



Noha Amaly<sup>1,2,3</sup>, Georges Istamboulie<sup>1,2</sup>,  
Ahmed Y El-Moghazy<sup>1,2,3</sup>  and Thierry Noguer<sup>1,2</sup>

## Abstract

The preparation of efficient molecularly imprinted polymers materials (MIPs) for pharmaceutical residue removal is still a challenging task. Herein, we design uniformly molecularly imprinted polymer nanospheres via a precipitation polymerization method using methacrylic acid (MAA) as functional monomer and *N,N*-methylenebis(acrylamide) (MBAA) as a crosslinker for removal of diclofenac (DFC) as a model for pharmaceutical pollutants. Nanospheres with average size 200 nm were prepared with MAA:MBAA at a ratio of 1:7 and acetonitrile/toluene (1:1) as a porogenic solvent. The successful synthesis is evidenced by Fourier transform infrared spectroscopy, scanning electron microscopy, and with a particle size analyzer. The rebinding experiments confirmed that the more introduction of the carboxyl groups from MAA could remarkably improve the imprinting effect with a significantly increased imprinting factor and specific rebinding capacity reached 450 mg/g after 15 min. Furthermore, the adsorption capacity of the molecularly imprinted polymers is maintained above 85% after seven regeneration cycles, indicating that the molecularly imprinted polymers can be used multiple times. Moreover, the developed molecularly imprinted polymers show promising DFC removal efficiency from real water samples, which suggests that the prepared molecularly imprinted polymer nanospheres are promising in DFC separation.

## Keywords

Molecularly imprinted polymers, methacrylic acid, precipitation polymerization, diclofenac, water samples

Date received: 20 February 2020; accepted: 22 April 2020

## Introduction

More than 80 pharmaceutical compounds have been identified in sewage effluents, surface water, groundwater, and food.<sup>1,2</sup> These compounds are of great concern because of their potential impact even at low concentration levels, on human health and the environment. Diclofenac (DFC) or 2-[2-(2,6-dichloroanilino)phenyl]acetic acid is one of the most important examples of non-steroidal anti-inflammatory drugs (NSAIDs).<sup>3</sup> It is widely used to reduce inflammation and as analgesic in cases of arthritis or acute injury.

Due to its extensive use, DFC is found in large quantities in wastewater, and is frequently detected in drinking water.<sup>4</sup> Wastewater treatment plants depend mainly on traditional removal techniques such as ozonation, UV irradiation, and activated carbon adsorption. However, these methods have been shown to be not very effective for DFC removal and some toxic and hazardous by-products may be formed during the treatment processes.<sup>5</sup> They originate mainly from human and veterinary usage and can be released, for example, after passing through sewage treatment plants.<sup>6</sup> From an analytical aspect, diclofenac and other pharmaceuticals

<sup>1</sup>Biocapteurs-Analyse-Environnement, University of Perpignan Via Domitia, Perpignan, France

<sup>2</sup>Laboratoire de Biodiversité et Biotechnologies Microbiennes, USR 3579 Sorbonne University (UPMC) Paris 6 et CNRS Observatoire Océanologique, Banyuls-sur-Mer, France

<sup>3</sup>Polymeric Materials Research Department, Advanced Technology and New Materials Research Institute, City of Scientific Research and Technological Applications (SRTA-City), New Borg El-Arab City, Egypt

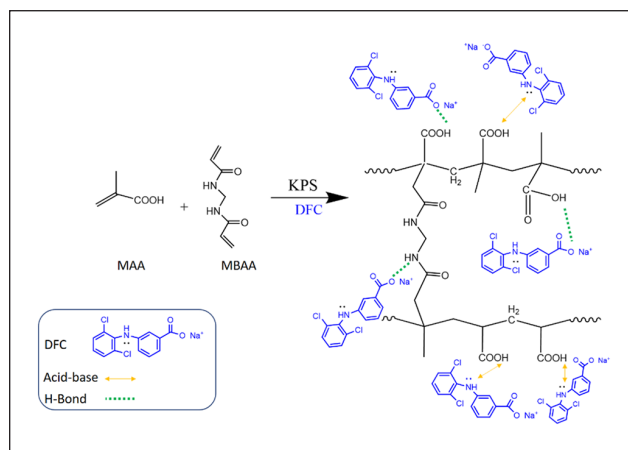
## Corresponding authors:

Ahmed Y El-Moghazy, Polymeric Materials Research Department, Advanced Technology and New Materials Research Institute, City of Scientific Research and Technological Applications (SRTA-City), Universities district, New Borg El-Arab City 21934, Alexandria, Egypt.  
Email: aelmoghazy1@gmail.com

Thierry Noguer, Biocapteurs-Analyse-Environnement, University of Perpignan Via Domitia, Perpignan 66000, France.  
Email: noguer@univ-perp.fr



are conventionally determined using high-performance liquid chromatography. However, solid-phase extraction is mandatory as a clean-up and pre-concentration technique prior to analysis of environmental samples. In the last two decades, extensive research efforts have been devoted to the fabrication and development of polymeric matrix as adsorbents or in form of molecularly imprinted polymers (MIPs) with specific recognition ability.<sup>7,8</sup> MIPs can be considered as good alternatives to classical solid-phase supports, both for removal and analytic purposes.<sup>9</sup> The molecular imprinting technique (MIT) involves the synthesis of a polymer in the presence of a template molecule.<sup>10</sup> Removal of the template molecule leads to “memory” sites, which are able to selectively rebind the original template contained in a complex mixture. These tailor-made polymers present the advantage of being highly selective for their template, they are easy to prepare and can be regenerated for multiple utilization, and assembling of the monomer molecules around the template can be achieved by non-covalent interactions such as hydrogen bonds, ion pairs, and hydrophobic interactions, or via reversible covalent interactions. The covalent approach usually provides better defined cavities with higher selectivity, whereas the non-covalent approach is more flexible and easier to apply because no chemical derivatization is required.<sup>6</sup> Functional monomers are chosen to interact with the template molecule since the formation of a stable template-monomer complex is fundamental for the success of molecular recognition.<sup>11</sup> Many successful methods have been developed to synthesize uniformly sized, spherical MIP beads such as suspension polymerization and emulsion polymerization.<sup>12</sup> Precipitation polymerization is a method of preparation of polymeric microspheres with sufficient control of product morphology, with sizes ranging between nanometer and micrometer range.<sup>13</sup> The advantages of this method include simplicity of preparation, no requirement for stabilizers or other additives, compatibility with high degrees of crosslinking agents, and the use of polar aprotic solvents as porogens which are capable of preserving non-covalent interactions between the template and the monomer. These advantages have made this method widely employed for the preparation MIP microspheres in molecular imprinting.<sup>14</sup> Hence in this research, the MIPs are formed by precipitation polymerization using DFC as the template and MAA as a functional monomer. The most widely applied technique is the non-covalent molecular imprinting method, which has many advantages, such as simple preparation, easy removal of the template, and fast rebinding kinetics. MAA is a commonly used functional monomer in non-covalent imprinting, having excellent ability to interact with the amine group of DFC.<sup>15</sup> MBAA was used as a crosslinker to favor the formation of poly(methacrylic acid) (P(MAA)). The produced MIP was characterized by Fourier transform infrared spectroscopy (FTIR) and scanning electron microscopy (SEM), and the removal efficiency of MIP was evaluated. Different factors affecting the adsorption efficiency were studied including the nature of the porogen solvent as well as the crosslinker and monomer concentrations. The effect of pH, DFC, and MIP dose were also investigated. Finally, the kinetic and isotherm behavior



**Scheme 1.** Reaction mechanism between MAA monomers with MBAA crosslinker and illustration of main interactions with DFC for MIPs preparation.

were studied for imprinted (MIP) and non-imprinted (NIP) polymers to predict the mechanism of adsorption process. The developed MIP was tested for diclofenac removal from different real water samples.

## Results and discussion

### Characterizations

**FTIR analysis.** MAA was chosen as functional monomer due to its acid functionality that could interact with the DFC molecules through hydrogen bonding and acid–base interaction between acidic carboxylate groups and basic ( $-N-$ ) lone pair of the DFC as illustrated in (Scheme 1). Moreover, the hydrophilic nature of the MAA helps to improve material wetting in water medium.<sup>16</sup> The effective polymerization of the MAA with MBAA crosslinker and even successful DFC adsorption were confirmed by FTIR spectra (Figure 1). Aforementioned, MAA forms H-bond with MBAA which is evidence by deformation of characteristic hydroxy broad band group ( $-O-H$ ) of a carboxylic acid in a PMAA chain<sup>17</sup> at  $3500\text{ cm}^{-1}$  due to H-bond formation with crosslinker  $N-H$  groups.<sup>18</sup> The appearance of new peak at  $1674\text{ cm}^{-1}$  which corresponds to  $C=O$  stretching in carboxamide in MBAA,<sup>19</sup> and the peak at  $1200\text{ cm}^{-1}$  for both the NIP and the MIP is for  $-C-N$  bond formed between MBAA and MAA. The appearance of characteristic peaks for DFC sodium salt at  $1572$  and  $995\text{ cm}^{-1}$  for the  $-C=O$  and  $C-Cl$  bonds, respectively,<sup>20</sup> indicates tethering of the DFC as a template in the MIP structure.

**SEM.** The morphologies of the MIPs and NIPs have been observed by SEM. As shown in Figure 2(a) and (b), significant differences were observed between the surfaces of NIP (Figure 2(a)) and MIP (Figure 2(b)). It was found that the MIPs and NIPs showed regular spherical particles ranging from 160 to 300 nm for NIP (Figure 2(a) and (c)). Their nanospherical shape is due to the nature of the charged MAA monomer that produces spherical polymer particles.<sup>21,22</sup> This spherical nature increases the adsorption surface and therefore creates more binding sites for DFC molecules. The

increase in the MIP size than NIPs is due to adsorption of the DFC on its surface.<sup>21</sup> The corresponding size distribution is displayed in (Figure 2(c) and (d)).

### Effect of the porogen solvent

The porogenic solvents used during the polymerization method have a great impact on the formation of specific cavities for the template. The uptake of DFC by MIPs prepared in different porogenic solvents/ratios was studied. It was clearly shown that the uptake efficiency increased by

decreasing the dielectric constant of the porogenic solvent (dielectric constants of water, acetonitrile, chloroform, and toluene are, respectively, 80, 37, 4.8, and 2.3). Using an initial DFC concentration of 100 mg/L, MIP B (water/MeCN, 1:1) showed only 15% DFC uptake, while MIP C (MeCN), MIP D (chloroform), and MIP A (toluene/MeCN, 1:1) retained, respectively, 21%, 29%, and 38% uptake of DFC. Changing to toluene/MeCN, 1:3, MIP E induced decrease in uptake to 20% as (Figure 3) illustrated. These results can be explained by the difference in the polarity of the solvent that affects interactions with the template molecule and functional monomer. These interactions strongly impact on the structure of the imprinting sites in the MIP. Solvents with high polarity display maximum interactions with both DFC and MAA, thus lowering their chance to interact to form appropriate imprinted sites. As observed in the case of MIP B, the use of a solvent mixture with a high dielectric constant and high polarity leads to a diminution of interactions between DFC and MAA.<sup>23</sup> Decreasing the solvent polarity as in the case of MIP A (using toluene) therefore leads to an increase in uptake efficiency.

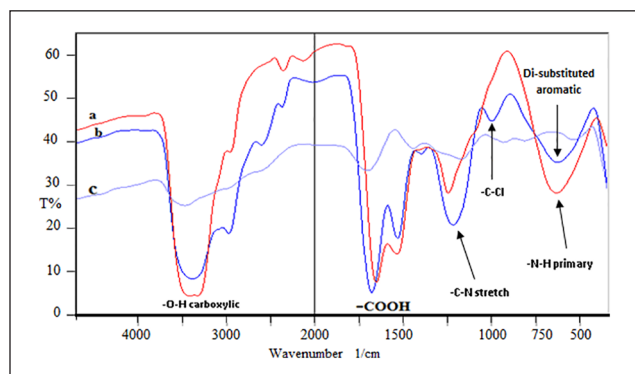


**Figure 1.** FTIR analysis for (a) NIP, (b) MIP before washing, and (c) PMAA.

### Effect of the crosslinker ratio

The effect of the crosslinker ratio was studied using MIPs prepared from the optimized porogen solvent mixture MIP (A) and different ratios between monomer and crosslinker,

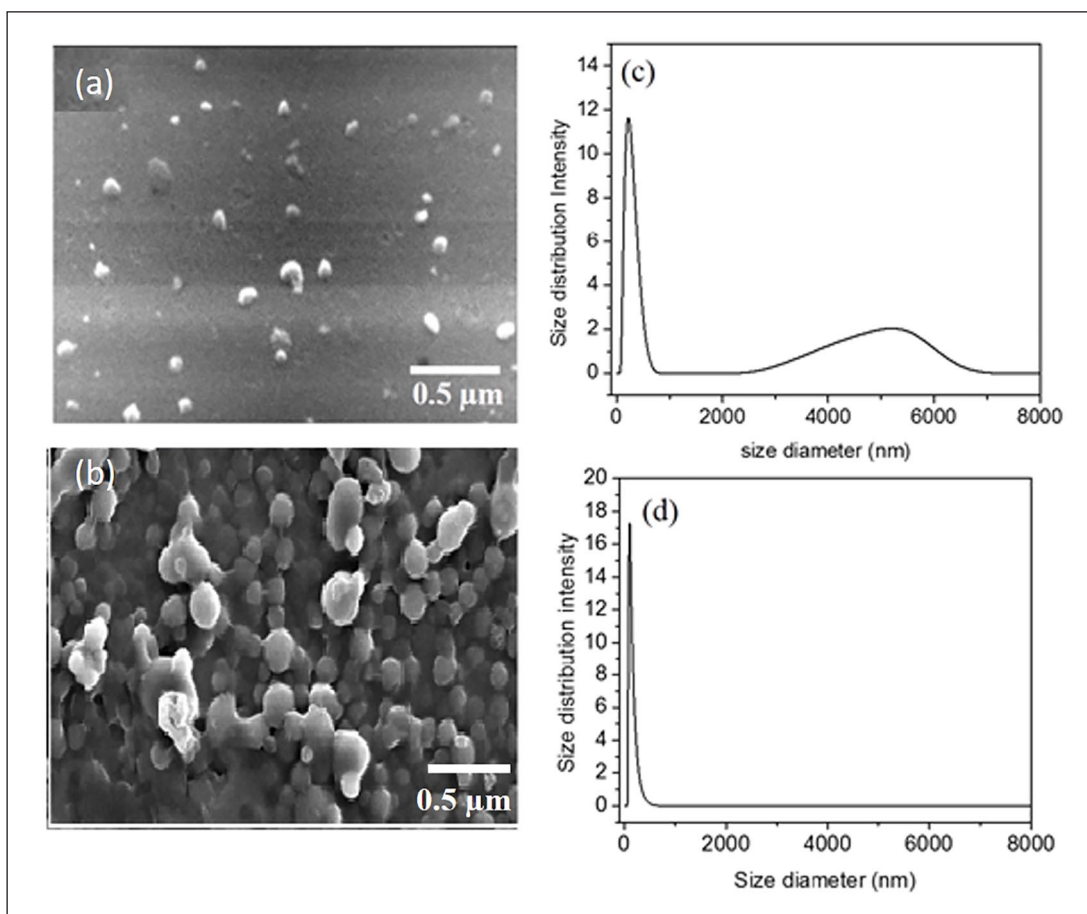


**Figure 2.** SEM images of PMAA-based (a) NIP, (b) MIP 7, and the diameter distributions of (c) MIP nanoparticles and (d) NIP nanoparticles.

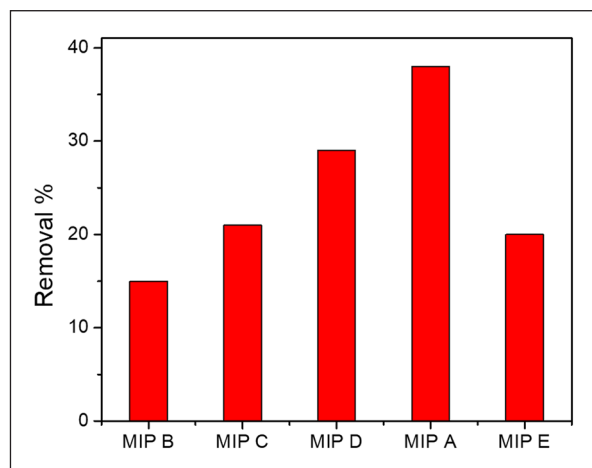


**Figure 3.** Effect of different co-solvent (porogen) ratio on DFC removal %.

1:2 (MIP 2), 1:3 (MIP 3), 1:5 (MIP 5), and 1:7 (MIP 7). Figure 4 shows that there was no significant difference in uptake efficiency by changing the crosslinker ratio between 2, 3, and 5; however, using a ratio of 1:7 resulted in an increase in the removal efficiency up to 85% from the initial DFC concentration of 100 ppm. These results can be explained by the increased stability of the cavities while increasing the degree of crosslinking, therefore enhancing the MIP binding capacity. High crosslinker ratios are preferred for obtaining pores with specific cavities complementary in both shape and chemical functionality even after removal of the template; they generally lead to materials with adequate mechanical stability that do not degrade after short times.<sup>24</sup> The MIPs prepared in this paper showed higher removal efficiencies than those based on 2-vinylpyridine as the functional monomer.<sup>5</sup>

#### Effect of pH on MIPs capacity

To illustrate the influences of buffer pH on the adsorption performance of MIP 7 and MIP 2, the pH value was regulated by utilizing 0.1 M NaOH and 0.1 M H<sub>3</sub>PO<sub>4</sub> solution, with results displayed in Figure 5. It remains relatively stable with very low capacity of 20% at extremely acidic medium (2–4) due the hydrophobic interaction with the DFC, whereas the removal efficiency improved by increasing the pH to reach maximum at pH range of 5.5–8. The removal efficiency reached a maximum at a pH range of 6–8 with around 85% removal efficiency. This is due to the MIP surface being negatively charged at pH > 5, at which the pK<sub>a</sub> for MAA is 4.6, which leads to electrostatic interactions with the DFC molecules. Also, the binding energy of the selectivity sites on MIP decreased in this pH range. The removal efficiency decreased at pH > 8 due to repulsive interactions between negative DFC molecules at pH > 7 and MIP.<sup>5</sup> These results suggest that the main interactions between DFC and MAA were related to hydrogen bonds or electrostatic forces.<sup>15</sup> It was also found that the MIP had higher adsorption efficiency than the NIP over the entire pH range investigated, showing a good imprinting effect and adsorption performance.

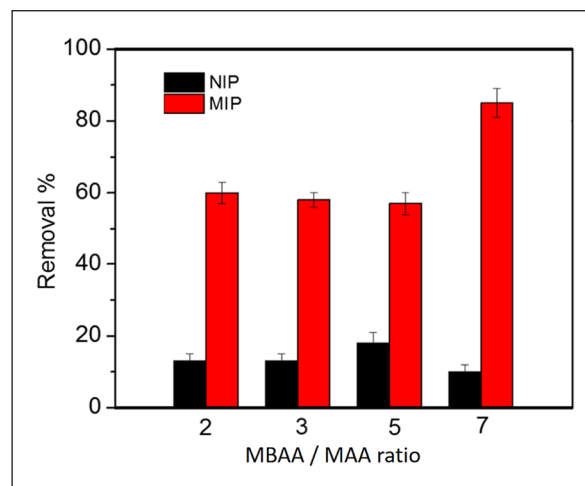


**Figure 4.** Effect of different crosslinker ratios on DFC removal efficiency, with DFC initial concentration of 100 ppm and pH 7 within 30 min adsorption time.

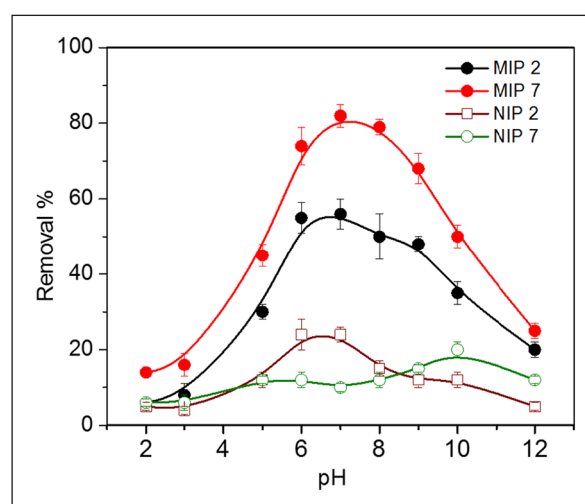


**Figure 5.** Effect of pH on DFC removal efficiency, with contact time of 30 min and DFC initial concentration of 100 ppm.

#### Effect of contact time

Figure 6 shows the effect of contact time on the uptake capacity of the MIPs and NIPs fabricated using crosslinker/monomer ratios of 1:2 and 1:7. The contact time between the polymer (0.5 mg/mL) and DFC (10 mL, 100 mg/L) was varied from 10 to 120 min. For both MIPs, it was found that the removal ratio increased rapidly and reached a plateau after 20 min. This fast adsorption rate may be due to the availability of a huge number of unoccupied binding sites on the MIPs, allowing the DFC to quickly reach the imprinted sites during the rebinding step. After 20 min of contact, no significant difference in removal efficiency was observed, suggesting that at this stage the imprinted sites for DFC molecules were fully saturated via a faster adsorption kinetic performance with adsorption rates of 0.05 and 0.02 g/mg<sup>-1</sup> min for MIP 7 and MIP 2, respectively. As expected, NIPs showed very low uptake DFC due to the fact that uptake depends only on adsorption.

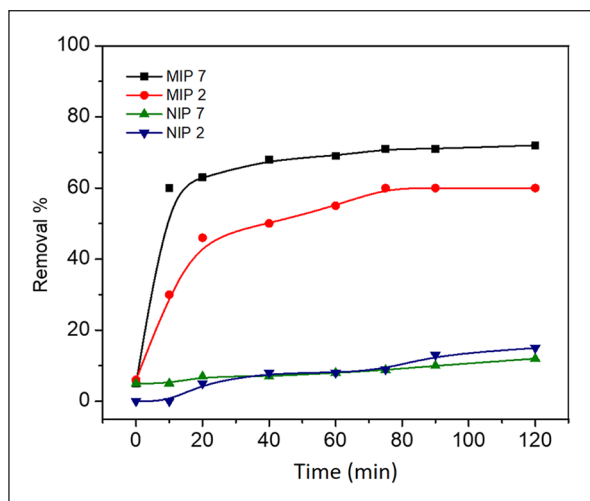


**Figure 6.** Effect of the contact time on the adsorption capacity at pH 7, with DFC initial concentration of 100 ppm.

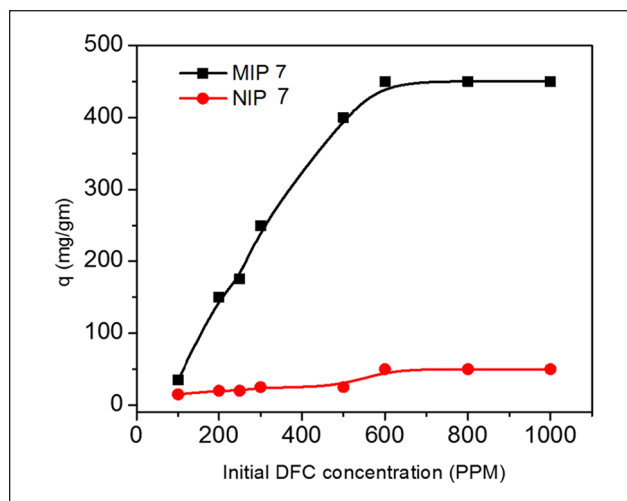


**Figure 7.** Effect of the initial DFC concentration on removal %, with 10 mg of MIPs in 20 mL of DFC at pH 7 for 30 min.

### Effect of the DFC initial concentration

Figure 7 shows the amount of DFC bound to the MIPs and NIPs at various initial concentrations. The adsorption capacities  $q$  (mg/g) of MIP 7 were much higher than those of the corresponding NIP 7 for each of the different initial concentration values of DFC. NIP showed an increase in the adsorption capacity with increase in the DFC initial concentration due to non-specific (due to the absence of specific cavities in the shape and size of DFC) rebinding in the NIPs due to hydrogen bonds and van der Waals forces between the template and the residual functional groups in the nanoparticles. The adsorption capacity of MIPs at higher initial concentrations (300-1000 ppm) is 2 times higher than reported previously (150 mg/g)<sup>5</sup> and more than 2 times data reported (125 mg/g) at same initial DFC concentration (300 ppm).<sup>25</sup> MIP 7 shows an improvement in adsorption capacities due to the nano size of the MIP particles, which have high surface area for adsorption per 1 g of MIP. Another reason is the hydrophilicity of MAA that increases the diffusion for soluble DFC into its particles. All these factors lead to a high  $q$  value that reaches up to 250 mg/g in the case of a 300 ppm initial concentration and 500 mg/g at an initial concentration 800 ppm. In this research, we studied the adsorption for the lowest initial concentration of 100 ppm so that it can be used in a wide range of applications.

### Adsorption kinetics

Kinetic studies were performed to calculate the adsorption rate and the equilibrium constant of the DFC uptake process. Pseudo-first-order and pseudo-second-order equations (1) and (2), respectively, based on the adsorption equilibrium capacity were considered:

Pseudo-first-order equation

$$q_t = q_c \left( 1 - \frac{1}{te^{k_1 t}} \right) \quad (1)$$

Pseudo-second-order equation

$$q_t = \frac{k_2 q_c^2}{1 + k_2 q_c} t \quad (2)$$

where  $k_1$  ( $\text{min}^{-1}$ ) and  $k_2$  ( $\text{mg/L min}$ ) are the rate constants of the pseudo-second- and pseudo-first-order adsorptions, respectively;  $q_t$  denotes the amount of DFC adsorption (mg/g) at time  $t$  (min); and  $q_c$  denotes the amount of DFC adsorption (mg/g) at equilibrium.

The plot of  $t/q$  versus  $t$  should result in a straight line if second-order kinetics are applicable, and then, the values of  $q_c$  and  $k_2$  can be calculated from the slope and the intercept of the plot, respectively. Adsorption experiments were carried out with 0.5 mg/mL of MIP 2 and MIP 7 for the adsorption of 100 mg/L of DFC solution. As shown in Figure 8, the kinetics of the adsorption process were followed well with the pseudo-second-order kinetic model leading to the higher correlation coefficients ( $R^2=0.99$ ) and confirming that DFC adsorption by MIPs fabricated with different crosslinker ratios or different solvent mixtures follows a pseudo-second-order reaction. The excellent straight line relation for pseudo-second-order kinetics gives an indication on the rate limiting chemisorption step,<sup>26</sup> suggesting that adsorption occurs through electrostatic interactions, ion exchange, or H-bonding. From pseudo-second-order kinetics (Table 1),  $q_c$  for MIP 7 was 35 mg/g, which has a higher capacity than MIP 2 (30 mg/g) and also has a faster adsorption rate of  $0.05 \text{ min}^{-1}$ . This is due to formation of more cavities, which shows the higher capacity in short time compared with those based on lower crosslinker ratio.

### Adsorption isotherms

Adsorption isotherms were studied to describe the interactive behavior between the adsorbate (DFC) and the adsorbent (polymer). Isotherm data analysis is important for estimating the adsorption capacity and for describing the adsorbent surface properties and affinity.<sup>15</sup> The Freundlich isotherm model is most frequently employed to describe

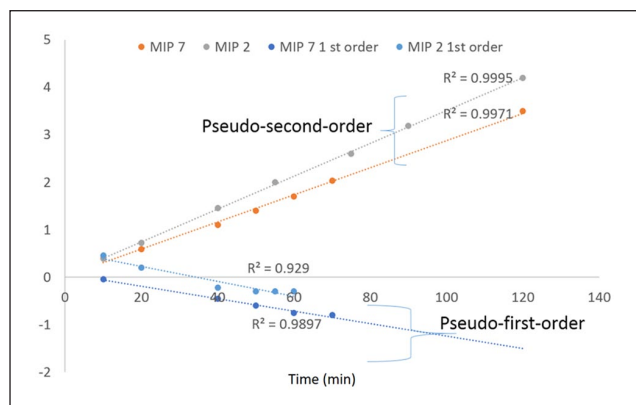


**Figure 8.** Second-order kinetic plot for the adsorption of DFC by different MIPs (10 mg of MIPs in 20 mL of 100 mg/L DFC at pH 7).

**Table 1.** Constants for the pseudo-first-order and pseudo-second-order kinetics for MIP 2 and MIP 7.

Pseudo-first-order kinetics			Pseudo-second-order kinetics					
MIP 2		MIP 7	MIP 2		MIP 7			
$q_e$	$k_1$	$R^2$	$q_e$	$k_2$	$R^2$	$q_e$	$k_2$	$R^2$
3.6	0.015	0.929	1.18	0.013	0.989	33	0.02	0.999

MIP: molecularly imprinted polymers.

adsorption onto heterogeneous surfaces from aqueous solution and reversible adsorption, which is not restricted to monolayer formations. It can be expressed in linear form by the following equation

$$\text{Log } q_e = \text{log } K_F + 1/n \text{ log } C_e$$

where  $K_F$  and  $1/n$  are the Freundlich constants related, respectively, to the adsorption capacity and the adsorption intensity of the adsorbent. A favorable adsorption is expected when  $1 < n < 10$ , which is even very favorable when  $1/n < 1$ .

The Langmuir isotherm model is predicated on the postulation that the structure of the adsorbent is homogeneous, where all adsorption sites are similar and energetically equivalent. The general Langmuir equation is given as

$$\frac{C_e}{q_e} = \frac{1}{q_m b} + \frac{C_e}{q_m}$$

where  $C_e$  is the equilibrium concentration of the DFC ( $\text{mg L}^{-1}$ );  $q_e$  is the equilibrium adsorption capacity ( $\text{mg g}^{-1}$ );  $b$  is the Langmuir adsorption constant ( $\text{L mg}^{-1}$ ); and  $q_m$  is the maximum adsorption amount ( $\text{mg g}^{-1}$ ), which can be obtained from the slope and intercept of the plot of  $C_e/q_e$  versus  $C_e$ . The applicability of each isotherm model was studied by judging the correlation coefficient values (Table 2). Using the Langmuir model, the correlation coefficient of the obtained representations was, respectively, equal to 0.99 and 0.30 for MIP 2 and MIP 7. The behavior of MIP 2

**Table 2.** The Langmuir and Freundlich constants values obtained for MIP 2 and MIP 7 (pH 7, 10 mg of MIP in 20 mL of DFC solution at  $100 \text{ mg L}^{-1}$ , contact time of 1 h).

Langmuir			Freundlich					
MIP 2		MIP 7	MIP 2		MIP 7			
B	$q_m$	$R^2$	B	$q_m$	$R^2$	$K_F$	n	$R^2$
1.2	1.6	0.99	0.05	5.5	0.34	1.5	1.25	0.85
			3.9	2.5	0.98			

MIP: molecularly imprinted polymers.

appeared to fit better with the Langmuir model, revealing the presence of homogeneous binding sites mainly on the surface of MIP 2. In contrast, MIP 7 fitted more clearly with the Freundlich model ( $R^2=0.98$ ), showing heterogeneous adsorption<sup>27</sup> that may be due to the more porous structure of MIP 7.

### Regeneration of MIPs

The removal efficiency for MIP 7 was tested by performing consecutive adsorption tests, with intermediate washing with methanol/acetic acid (9:1, v/v). This test is crucial for demonstrating the possible reusability of the MIPs. It was shown that MIP 7 displayed a constant efficiency over seven adsorption–desorption cycles; the removal efficiency keeps 85% of the initial efficiency after seven cycles (Figure 9). The efficiency decreased at cycle 8 to reach 46% in both cases. This decrease in uptake may be explained by progressive saturation of the MIP active sites that leads to the prevention of more template uptake.

### Specificity of the developed MIPs

To investigate the selective efficiency, the adsorption properties of the MIP were tested by comparing DFC adsorption capacity with that of carbamazepine (CBZ) at the same concentration of 500 ppm. CBZ was selected due to its structure is similar to DFC at a certain extent and it also widely coexists with DFC in water bodies. The mixture was mixed with the MIPs nanoparticles for 30 min. Next, the compounds in both the washing and elution fractions were analyzed by high-performance liquid chromatography (HPLC). Although the binding capacity of NIP for the DFC is lower than CBZ, the adsorption efficiency of MIPs with the DFC was two times higher than the CBZ (Figure 10), which confirm the presence of specific imprinting sites in size, 3D structure, and complementary chemical bonds that improve the adsorption of the target molecule and reduced the binding of the interfering compound. CBZ was unable to bind as strongly as the DFC because its size cannot match the DFC memory cavities and its functional group position does not correspond to the functional groups in the cavities.<sup>28</sup> The non-specific adsorption mechanisms could be due to the hydrophobic nature of the polymers. The solvent washing is therefore recommended to remove non-specifically bound interferences and to strengthen or leave unaffected, the specifically bound substances.<sup>5</sup>

### Applicability of the developed MIPs

In order to evaluate the applicability of the developed MIPs for removal of DFC from water, simulated water samples from different sites were collected and spiked with DFC to be used as simulated real water samples. Water samples were collected from Lac de Villeneuve de

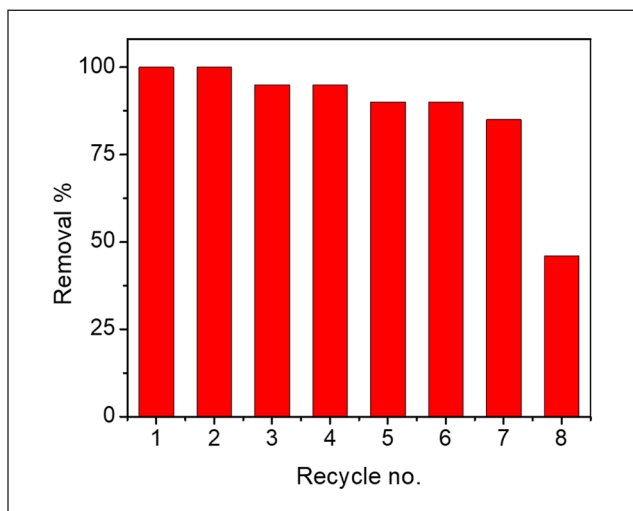


**Figure 9.** MIP 7 adsorption efficiency for DFC after various regeneration cycles by 10 mg MIP 7 in 20 mL DFC at pH 7 for 30 min.

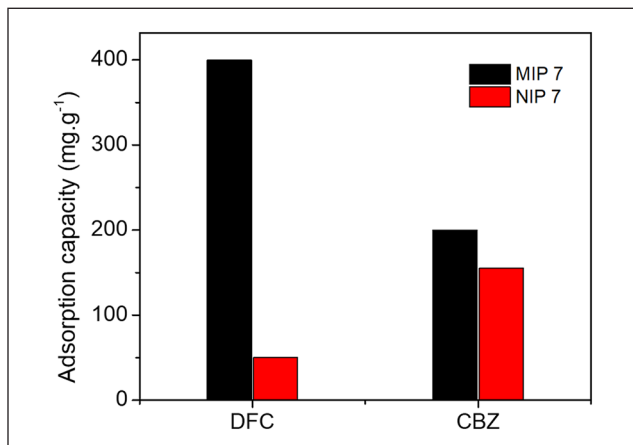


**Figure 10.** Adsorption performance during 30 min via NIP and MIP toward DFC and CBZ at pH 7.

la Raho (Pyrénées-Orientales, France) and the Nile River (Rosetta branch, Egypt). The water samples were first analyzed by high-performance liquid chromatography–mass spectrometry (HPLC-MS) for confirming the absence of DFC. Water samples were spiked with various DFC concentrations of 50, 100, and 150 ppm. The experiments were run using 0.5 mg/mL of MIP 7 for 15 min for removal of initial DFC concentrations from 20 mL of the sample. Each measurement was carried out in triplicate. Table 3 shows the obtained results for each sample after the removal process. The developed MIPs' efficiency improved by initial DFC increase, recording about 83% removal from the different water samples with an initial concentration of 150 ppm. The performance of the developed MIPs for DFC removal from the real sample was very good, and there was no significant difference in the removal efficiency compared with that when using distilled water.

### Conclusion

Precipitation polymerization was successfully employed for generating molecularly imprinted polymeric microspheres specific for diclofenac. A significant difference in uptake capacity was observed between NIP and MIP, which can be explained by the formation of specific cavities and chemical bonds by self-assembling of monomers around a DFC template. The presence of such cavities was clearly evidenced by SEM, and the formation of specific bonds between the monomer and DFC was evidenced by FTIR analysis. The efficiency of MIP was shown to be strongly affected by the crosslinker/MAA (monomer) ratio and by the nature of the porogenic solvent. It was shown that the use of a less polar solvent (MeCN/toluene, 1:1) and a crosslinker/monomer ratio higher than 1:5 resulted in high adsorption capacity, reaching 82% of removal of DFC even after seven regeneration cycles. The optimized MIPs described in this paper showed high differences in the removal efficiency between MIPs and NIPs, reaching more than 75%. Furthermore, the developed MIPs were successfully used for the removal of DFC from simulated real water samples collected from different sources (France and Egypt). Finally, the regeneration and short time needed to remove more than 80% of DFC suggests that the prepared MIP can be applied in applications for high-efficiency DFC removal.

**Table 3.** Removal efficiency of MIP 7 various water samples spiked with 50, 100, or 150 ppm of DFC.

Initial DFC concentration (ppm)	Distilled water		Lake Raho sample		Nile river sample	
	Concentration removed (ppm)	Removal %	Concentration removed (ppm)	Removal %	Concentration removed (ppm)	Removal %
50	37.5	75	36	72.2	35.5	71
100	80	80	80	80	79.4	79.4
150	127.5	85	124.5	83	125.8	83.9

MIP: molecularly imprinted polymers.

## Experimental

### Materials

Methacrylic acid (MAA) monomer, *N,N*-methylenebis (acrylamide) (MBAA), potassium persulfate (KPS), and diclofenac sodium salt (DFC) were purchased from Fluka (Switzerland). Solvents and co-solvents—toluene, acetonitrile, chloroform, and ethanol—were purchased from Sigma Aldrich (Germany) and were analytical reagent grade. These reagents were used without any further purification.

### Preparation of MIPs and NIPs

The MIP was prepared via precipitation polymerization, in which 0.79 mmol (250 mg) template molecule DFC dispersed with the functional monomer MAA (5 mmol) in 20 mL of acetonitrile (MeCN) in a round bottom flask. Subsequently, the crosslinker MBAA (10 mmol) was added to monomer mixture and stirred over 30 min. After adding of the radical initiator KPS (0.01 mmol), the reaction mixture was degassed with a gentle flow of N<sub>2</sub> for 5 min, sealed under N<sub>2</sub> and placed in a silicon oil bath at 70 °C for 4 h to carry out the polymerization process. The resulting polymer was precipitated by acetone, and the obtained white polymer particles were collected by centrifuge at 15,000 r/min for 15 min, dried at 70 °C and grounded to crush any coagulated particles. Finally, the template and the non-polymerized compounds were extracted simply by washing the polymer powders with methanol/acetic acid solution (9:1, v/v), and this procedure was repeated three times. Then, the polymer was dried overnight at 55 °C. The corresponding non-imprinted polymer prepared with the same procedure just in the absence of the DFC molecule. The optimum MIPs particle size and removal efficiency were obtained by different MAA:MBAA ratio ranges from 1:2 to 1:7 for various co-solvents (toluene, chloroform, water, or acetonitrile) with different ratios as illustrated in Table 4 for template removal.

The presence/absence of DFC in washing solvent was estimated after each run by UV analysis at 275 nm using DFC calibration curve starting from 25 to 1100 ppm concentration.

### Characterization

MIPs and NIPs were characterized by FTIR using a Shimadzu FTIR-8400S (Shimadzu, Japan). SEM was performed using a Joel JSM 6360LA SEM (JEOL, Japan) instrument by placing samples on a metal stub and coating with gold using an ion sputter under vacuum to measure particle size by submicron particle size analyzer (Beckman Coulter, USA). The NIP and MIP nanoparticles were dispersed in water using a vortex for 5 min to be sure that all the particles had been dispersed, at a temperature 20 °C.

### Adsorption studies

The effects of pH and contact time were examined. Solutions of 0.1 N hydrochloric acid (HCl) or 0.1 N sodium

**Table 4.** The co-solvent and monomer/crosslinker ratio for MIP synthesis.

MIP name	Co-solvent	MAA/MBAA
B	Water:MeCN 1:1	1:7
C	MeCN	1:7
D	Chloroform	1:7
A	Toluene/MeCN (1:1)	1:7
E	Toluene/MeCN (1:3)	1:7
2	Toluene/MeCN (1:1)	1:2
3	Toluene/MeCN (1:1)	1:3
5	Toluene/MeCN (1:1)	1:5
7	Toluene/MeCN (1:1)	1:7

MIP: molecularly imprinted polymers.

hydroxide (NaOH) were used for adjusting the pH value from 2 to 12. MIP (0.5 mg/mL) was added to a DFC initial concentration of 100 ppm dissolved in distilled water, and the contact time between MIP and DFC was varied from 10 to 120 min. The concentration of DFC after adsorption was determined via detecting the absorbance intensity changes of the solutions at 275 nm by UV-Vis spectrophotometry (Evolution 600, Thermo), using a quartz cell with a length of 1 cm, and pure distilled water as the blank sample.

### Kinetic studies

Kinetic studies of DFC adsorption allowed evaluation of the adsorption rate and equilibrium constant for the DFC uptake process. The binding efficiency of the synthesized MIPs was measured as a function of time. Adsorption kinetics were established using 0.5 mg/mL of MIP and a 100 ppm DFC initial concentration in a 1:1 toluene:MECN co-solvent/10 mL mixture. The residual DFC concentration was measured at different times until equilibrium, which was reached after 120 min. The DFC uptake at different times, defined as the adsorption capacity  $q_e$  (mg/g), was calculated using equation (3)

$$q_e = (C_0 - C_t) V / m \quad (3)$$

where  $C_0$  is the initial DFC concentration (ppm),  $C_t$  is the DFC concentration at equilibrium (ppm),  $V$  is the volume of the solution (L), and  $m$  (g) is the mass of MIP.

### Isotherm studies

Studies of the adsorption equilibrium isotherm are useful for determining the mechanism of DFC uptake. The uptake capacity of 10 mg of MIPs was thus tested using various initial concentrations of DFC (16, 20, 32, 40, 50, 60, 80, and 160 ppm) in distilled water at pH 7 for a contact time of 120 min, and the residual DFC concentration was determined, allowing the calculation of data for the Freundlich and Langmuir isotherms.

### Regeneration of MIPs

10 mg of MIPs were mixed with 20 mL of a DFC solution with an initial concentration of 100 ppm. The MIPs were

washed with methanol/acetic acid (9:1, v/v) until the template could not be detected in the filtrate. The MIPs were then washed with methanol, vacuum-dried, and reused until unsatisfactory DFC removal was obtained.

### Applicability of MIPs

Under the optimum conditions, the application of the developed MIPs for the removal of diclofenac from the real samples was investigated with simulated water samples from different sources, which were spiked with known concentrations of diclofenac.

### Declaration of conflicting interests

The author(s) declared no potential conflicts of interest with respect to the research, authorship, and/or publication of this article.

### Funding

The author(s) disclosed receipt of the following financial support for the research, authorship, and/or publication of this article: This work was supported by the French Government through a fellowship granted by the French Embassy in Egypt (Institut Français d'Égypte).

### ORCID iD

Ahmed Y El-Moghazy  <https://orcid.org/0000-0002-1083-4282>

### References

1. Heberer T. *Toxicol Lett* 2002; 131: 5.
2. El-Moghazy AY, Zhao C, Istamboulie G, et al. *Biosens Bioelectron* 2018; 117: 838.
3. Madikizela LM and Chimuka L. *J Environ Chem Eng* 2016; 4: 4029.
4. Cantarella M, Carroccio SC, Dattilo S, et al. *Chem Eng J* 2019; 367: 180.
5. Dai C-M, Geissen S-U, Zhang Y-L, et al. *Environ Pollut* 2011; 159: 1660.
6. Sun Z, Schüssler W, Sengl M, et al. *Anal Chim Acta* 2008; 620: 73.
7. Hemmati K, Sahraei R and Ghaemy M. *Polymer* 2016; 101: 257.
8. Amaly N, Si Y, Chen Y, et al. *Colloids Surfaces B Biointerfaces* 2018; 170: 588.
9. Wang X, Dong S and Bai Q. *Biomed Chromatogr* 2014; 28: 907.
10. Vasapollo G, Sole R, Del Mergola L, et al. *Int J Mol Sci* 2011; 12: 5908.
11. Masci G, Aulenta F and Crescenzi V. *J Appl Polym Sci* 2002; 83: 2660.
12. Fareghi AR, Moghadam PN and Khalafy J. *Starch* 2017; 69: 1.
13. Pardeshi S and Singh SK. *RSC Advances* 2016; 6: 23525.
14. Figueiredo L, Erny GL, Santos L, et al. *Talanta* 2015; 1.
15. Chaitidou S, Kotrotsiou O, Kotti K, et al. *Mater Sci Eng B Solid-State Mater Adv Technol* 2008; 152: 55.
16. Surikumaran H, Mohamad S and Sarih N. *Int J Mol Sci* 2014; 15: 6111.
17. Hassanzadeh-Khayyat M, Lai EPC, Kollu K, et al. *J Water Resour Prot* 2011; 3: 643.
18. Sadeghi M and Heidari B. *Materials* 2010; 4: 543.
19. Langer R and Zundel G. *J Chem Soc Faraday Trans* 1995; 91: 3831.
20. Zakaria ND, Yusof NA, Haron J, et al. *Int J Mol Sci* 2009; 10: 354.
21. Aiello PB, Borges FA, Romeira KM, et al. *Mater Res* 2013; 17: 146.
22. Liu Y, Zhang G, Deng L, et al. *Anal Methods* 2014; 6: 684.
23. Bompant M, Goto A, Waittraint O, et al. *Polymer* 2015; 78: 31.
24. Song X, Wang J and Zhu J. *Mater Res* 2009; 12: 299.
25. Yan H and Row KH. *Int J Mol Sci* 2006; 7: 5155.
26. Shen F, Zhang Q and Ren X. *Chem Commun* 2015; 51: 183.
27. Ho YS and McKay G. *Process Biochem* 1999; 34: 451.
28. Nicolescu T-V, Sarbu A, Ghiurea M, et al. *UPB Sci Bull Ser* 2011; 73: 163.